Featured Article

Response of the protozooplankton assemblage during the European Iron Fertilization Experiment (EIFEX) in the Antarctic circumpolar current

PHILIPP ASSMY[1,2]*, BORIS CISEWSKI[3], JOACHIM HENJES[4], CHRISTINE KLAAS[2], MARINA MONTRESOR[5]
AND VICTOR SMETACEK[2]

[1]NORWEGIAN POLAR INSTITUTE, FRAM CENTRE, 9296 TROMSO, NORWAY, [2]ALFRED WEGENER INSTITUTE HELMHOLTZ CENTER FOR POLAR AND MARINE RESEARCH, 27570 BREMERHAVEN, GERMANY, [3]THÜNEN INSTITUTE OF SEA FISHERIES, PALMAILLE 9, 22767 HAMBURG, GERMANY, [4]IMARE—INSTITUTE FOR MARINE RESOURCES GMBH, 27570 BREMERHAVEN, GERMANY AND [5]STAZIONE ZOOLOGICA ANTON DOHRN, 80121 NAPOLI, ITALY

*CORRESPONDING AUTHOR: philipp.assmy@npolar.no

Ocean iron fertilization experiments enable the quantitative study of processes shaping the structure and functioning of pelagic ecosystems following perturbation under *in situ* conditions. EIFEX was conducted within a stationary eddy adjacent to the Antarctic Polar Front over 38 days in February/March 2004 and induced a massive diatom bloom. Here, we present the responses in abundance and biomass of all identifiable protozooplankton taxa (heterotrophic protists ranging from 2 to 500 μm) during the bloom. Acantharia, dinoflagellates and ciliates together contributed >90% of protozooplankton biomass in the upper 100 m throughout the experiment with heterotrophic nanoflagellates, nassellaria, spumellaria, phaeodaria, foraminifera and the taxopodidean *Sticholonche zanclea* providing the remainder. Total protozooplankton biomass increased slightly from 1.0 to 1.3 g C m^{-2} within the fertilized patch and remained at 0.7+0.04 g C m^{-2} outside it. However, distinct trends in population build-up or decline were observed within the dominant taxa in each group. In general, smaller less-defended groups such as aloricate ciliates and athecate dinoflagellates declined, whereas the biomass of large, spiny and armoured groups, in particular acantharia, large tintinnids and thecate dinoflagellates increased inside the patch. We attribute the higher accumulation rates of defended taxa to selective, heavy grazing pressure by the large stocks of copepods. Of the defended taxa, acantharia had the lowest mortality rates and the highest biomass. Large stocks of tintinnid loricae in the deep water column identify this group as a relevant contributor to deep organic carbon export. Highest accumulation rates (0.11 day^{-1}) were recorded in *S. zanclea*.

KEYWORDS: protozoa; rhizaria; sarcodines; Southern Ocean; top-down control

INTRODUCTION

Plankton can be grouped into four broad categories: bacterio-, phyto-, protozoo- and metazooplankton based on their size ranges, functional roles (Sieburth *et al.*, 1978), and phylogeny (Adl *et al.*, 2012). Although all categories play fundamentally important roles in determining the structure and functioning of pelagic ecosystems (Strom, 2008), much less attention has been focused on protozooplankton (heterotrophic protists) ecology than on the other categories. Thus, although grazing by heterotrophic nanoflagellates (HNF) is known to be a major constraint in maintaining bacterial abundances at values around 10^6 mL^{-1} (Chow *et al.*, 2013; Pernthaler, 2005), little is known about abundance and dynamics of the HNF relative to production by their food source or to predation on them by larger microprotozooplankton. Similarly, field observations (Henjes *et al.*, 2007; Saito *et al.*, 2005) and *in vitro* feeding experiments (e.g. Strom *et al.*, 2007) indicate that the potentially major grazers of phytoplankton and HNF, ciliates and dinoflagellates, are kept in check by copepod grazing (e.g. Saiz and Calbet, 2011; Smetacek, 1981) but again, information on the dynamics of these groups in relation to bottom-up and top-down factors is limited. Heterotrophic dinoflagellates are able to graze on a large variety of different size classes depending on feeding behaviour. The thecate (armoured) dinoflagellates of the cosmopolitan genera *Protoperidinium* and *Dinophysis* can feed on prey much larger than themselves by either extruding a feeding membrane that can engulf entire diatom chains (pallium-feeding) in case of the former or by using an umbilical cord-like peduncle to pierce the prey (peduncle-feeding) in case of the latter (Jacobson, 1999). Athecate (naked) dinoflagellates can consume a wide range of prey items (Sherr and Sherr, 2007) and usually engulf prey of similar size (Jacobson and Anderson, 1986). However, exceptions have been reported (Saito *et al.*, 2006), suggesting that this group of protists has a high plasticity of feeding behaviours. Aloricate (naked) ciliates usually ingest prey smaller than themselves and are deterred by bristles and spines. The same applies to loricate ciliates (tintinnids), which are restricted to smaller prey dictated by the oral diameter of their lorica (Caron *et al.*, 2012; Dolan, 2010). The emerging view is that protozooplankton are capable of feeding on all marine phytoplankton, from pico-cyanobacteria to the largest diatoms and phototrophic dinoflagellates, and are potentially able to match or even exceed growth rates of phytoplankton (Fenchel, 1987; Finlay, 2001; Sherr and Sherr, 1994), with ciliates generally exhibiting higher growth rates than heterotrophic dinoflagellates (Hansen and Jensen, 2000; Strom and Morello, 1998). The fact that the biomass of phytoplankton blooms generally exceeds that of protozooplankton hence implies that the latter are not resource-limited (bottom-up) and hence must be controlled by mortality factors (top-down) which are largely attributed to selective predation by metazooplankton (Irigoien *et al.*, 2005; Sherr and Sherr, 2009), in particular copepods (Calbet and Saiz, 2005; Sherr and Sherr, 2007). An alternative but not mutually exclusive explanation for the occurrence of massive high-latitude phytoplankton blooms has been put forward by Rose and Caron (Rose and Caron, 2007), suggesting that low temperature exerts a stronger constraint on protozooplankton rather than on phytoplankton growth rates leading to a decoupling of the two and accumulation of phytoplankton biomass in high-latitude oceans.

Apart from these dominant protozoan groups, attention has also focused on members of the rhizaria (formerly classified under sarcodines; Caron and Swanberg, 1990), in particular the foraminifera and polycystine radiolarians. These groups are less abundant than ciliates and dinoflagellates but, in contrast to most other plankton species, their mineral skeletons preserve in the fossil record of the underlying sediments and are widely used as proxies in geochemical and micropaleontological studies (Abelmann and Gowing, 1997; Abelmann and Nimmergut, 2005; Katz *et al.*, 2010; Mutti and Hallock, 2003). Knowledge of the ecological traits of these species can therefore provide valuable information for proxy validation. Two other members within the rhizaria, the taxopodidan *Sticholonche zanclea* and acantharians, are less well studied because their opaline and celestite skeletons, made of silica and strontium sulphate, respectively, rapidly disintegrate (*S. zanclea*) and dissolve (acantharians) after cell death if not adequately preserved (Michaels *et al.*, 1995; Takahashi and Ling, 1980). This can lead to an underestimation of the role of these protists, as particularly acantharians can account for a significant fraction of protozooplankton biomass (Henjes *et al.*, 2007).

The ecology of the surface layer of the Antarctic Circumpolar Current (ACC) has a strong influence on ocean nutrient cycles because of the key role played by this water mass in driving deep ocean circulation (Sarmiento *et al.*, 2004). Satellite and field observations indicate that productivity is regulated by the supply of iron, and mesoscale iron fertilization experiments have shown that response patterns of natural assemblages to alleviation of the limiting resource can be tracked under *in situ* conditions (Boyd *et al.*, 2007). Therefore, ocean iron fertilization experiments present a powerful approach to study the relationship between structure and function of pelagic ecosystems in relation to biogeochemical processes (Smetacek and Naqvi, 2008). They are classic perturbation experiments that shift the ecosystem from a resource-limited state (in this case iron) to a

resource-replete one, thus enabling the study of the response patterns at the species level under natural conditions of bottom-up and top-down control. During EIFEX, we had the unique opportunity to follow, over 38 days, the protozooplankton assemblage in the upper 350 m of a coherent water mass inside a stationary eddy situated in the Polar Frontal Zone over the course of an iron-induced bloom (Smetacek *et al.*, 2012). The EIFEX bloom was dominated by various thin-shelled spiny and thick-shelled diatom species (Assmy *et al.*, 2013). After the third week, mass mortality triggered aggregate formation and rapid sinking to the deep ocean of the thin-shelled diatoms, while the thick-shelled species persisted in the surface layer (Assmy *et al.*, 2013). The aim of the present study was to investigate the response of the protozooplankton assemblage to the iron-induced bloom in comparison with unperturbed waters outside the fertilized patch by following the abundance and biomass of the various taxa in the water column.

METHOD

Study area and iron fertilization

EIFEX was conducted in the Atlantic Sector of the Southern Ocean (02°E, 49°S) in late austral summer (11 February–20 March 2004) during cruise ANT-XXI/3 of R/V *Polarstern* (Smetacek *et al.*, 2012). A circular patch of initially 167 km^2 was fertilized with dissolved Fe(II)-sulphate inside the clockwise-rotating core of an eddy formed by the meandering Antarctic Polar Front (APF). The in-patch stations were placed at the sites of highest photosynthetic efficiency (Fv/Fm) and chlorophyll concentrations and lowest pCO$_2$ values, hence closest to the centre of the iron-fertilized patch. Whereas in-stations sampled more or less the same water column throughout, out-patch stations sampled different water columns in relation to the location of the patch within the eddy. The first station, sampled one day prior to iron addition (day-1) was located in the centre of the circular patch that was subsequently fertilized.

Abundance

Water samples for enumeration of naked and thus more delicate protozooplankton, including HNF, aloricate ciliates and aplastidic athecate dinoflagellates, as well as aplastidic thecate dinoflagellates <20 μm were collected in 200 mL brown glass bottles at 10, 40 and 100 m depth at the initial station prior to iron addition (day-1) and at eight in-patch and five out-patch stations using Niskin bottles attached to the CTD rosette. Samples were preserved with acid Lugol's iodine solution at a final

concentration of 5% (vol/vol). Fixed samples were stored at 4°C in the dark until counting in the home laboratory. Samples were settled in 50 mL Utermöhl sedimentation chambers (Hydrobios, Kiel, Germany) for 48 h. Sodium thiosulphate was added to each sample to bleach the iodine solution and allow for autofluorescence detection.

For the quantitative assessment of large, shell- and mineral-bearing protozooplankton, including acantharia, the taxopodidan *Sticholonche zanclea*, phaeodaria, polycystines (composed of nassellaria and spumellaria), foraminifera, tintinnids and aplastidic thecate dinoflagellates >20 μm, water samples were taken from 8 to 15 discrete depths between 10 and 550 m at the pre-fertilization station and eight in-patch and five out-patch stations using Niskin bottles. The entire content of one or two Niskin bottles (12 or 24 L), depending on sampling depth, was gently passed through a 20 μm mesh plankton net and concentrated to a final volume of 50 mL. Special care was taken not to contaminate the concentrated samples with plankton collected from a previous CTD cast by thoroughly washing the plankton nets and tubes after each sample collection. The concentrated samples were preserved with hexamethylenetetramine-buffered formaldehyde solution at a final concentration of 2% (vol/vol) and stored at 4°C in the dark for subsequent counting. Two millilitres of strontium chloride solution were added to each sample to prevent dissolution of the acantharian celestite (strontium sulphate) skeletons by keeping the samples saturated with strontium. A volume of 3 mL (for samples collected between 10 and 150 m) and 10 mL (for the deep samples between 200–550 m) was settled in Utermöhl sedimentation chambers for 6–24 h depending on the settling volume. Prior to counting, 35 μL of stock solution of the nuclear fluorochrome 4′,6-diamidino-2-phenylindole (DAPI) (Porter and Feig, 1980) was added to each sample to stain the nucleus of the cells. Cells with stained nuclei were considered alive at the time of sampling. In addition to live cells, intact empty and damaged tintinnid loricae as well as acantharian, phaeodarian and polycystine skeletons were enumerated.

Towards the end of the experiment, full, empty and damaged tintinnid loricae were additionally sampled at 5 to 10 depths along the deep water column below 500 m at five stations: three inside the patch, one outside the patch and one at the margin of the patch (Supplementary data, Table SI). For the samples collected in the deep water column (>500 m), the content of a whole Niskin bottle (12 L) was concentrated down to 50 mL by pouring the water gently through 10-μm mesh. Cells were settled in 10–25 mL sedimentation chambers for 24 h.

All organisms were enumerated using inverted light and epifluorescence microscopy (Axiovert 135 and Axiovert

200, Zeiss, Oberkochen, Germany) within 18 months of collection according to the method illustrated by Throndsen (Throndsen, 1995). We followed the recent phylogeny by Krabberød et al. (Krabberød et al., 2011) that groups foraminifera, radiolaria including (1) polycystines (nassellaria and spumellaria), (2) spasmaria (acantharia and taxopodida, i.e. *Sticholonche zanclea*) and cercozoa (phaeodaria) within the super group rhizaria. HNF include choanoflagellates and unidentified flagellates counted in size classes of <10, $10-20$ and $>20\ \mu m$. Unidentified aloricate ciliates and athecate dinoflagellates were counted in size classes of <20, $20-40$, $40-60$ and $>60\ \mu m$. Acantharians, foraminifera, *S. zanclea* and thecate dinoflagellates $>20\ \mu m$ were further grouped in size classes smaller and larger than $50\ \mu m$ for more accurate biovolume calculation. Juvenile foraminifera and polycystines were differentiated from adult specimens by their smaller size, low number of chambers in the case of the former and incomplete silica skeletons in the case of the latter. An overview of all stations and depths sampled for protozooplankton with indication of number of individuals counted, cell abundances (cells L^{-1}) and $\pm 95\%$ confidence intervals for the abundance estimates can be found in Supplementary data, Tables SII–SV. We compared the slopes (b) of the in-patch and out-patch regression lines, with days since first iron release being the independent and standing stocks being the dependent variable, to ascertain whether significant differences between in-patch and out-patch trends exist. The null hypothesis H0 'in-patch and out-patch slopes are equal' was rejected based on an evidence level alpha <0.05 (Zar, 2010, Chapter 18).

Biomass

Biovolumes of aloricate ciliates, tintinnids, athecate and thecate dinoflagellates and the taxopodidan *Sticholonche zanclea* were estimated from dimensions of appropriate geometrical shapes of at least 30 randomly chosen individuals of each taxon. The biovolumes of foraminifera were determined by assuming a spherical shape and using the longest dimension across the calcite test as the diameter (Bè et al., 1977). Biovolumes of acantharia were calculated assuming a sphere, or a spheroid shape (Michaels et al., 1995). For adult phaeodarians and polycystines, the biovolume was measured as the diameter of the spherical central capsule (Michaels et al., 1995).

Cell volume of HNF, dinoflagellates and ciliates was converted to cellular carbon content through recommended conversion equations (Menden-Deuer and Lessard, 2000). The different members of the rhizaria were converted to biomass (carbon) using measured carbon:volume ratios of $0.08\ pg\ \mu m^{-3}$ for acantharia, $0.089\ pg\ \mu m^{-3}$ for

foraminifera and $0.01\ pg\ \mu m^{-3}$ for phaeodaria and polycystines (Michaels et al., 1995).

For each station, depth-integrated standing stocks (mg C m^{-2}) were calculated from the discrete depth profiles by trapezoidal integration of 3 to 5 depths for the upper 100 m, 6 depths for the upper 150 m, 7 to 8 depths for the upper 250 m and 8 to 10 depths for the upper 350 m. Accumulation rates inside the patch were calculated by estimating the slope of the regression for the log-transformed standing stock values over a time interval, covering at least four data points, in which an increase was recorded.

RESULTS

Protozooplankton standing stocks and composition

The protozooplankton during EIFEX was composed of a phylogenetically diverse assemblage of mineral- and shell-bearing and naked taxa spanning one order of magnitude in size (Supplementary data, Fig. S1). Out of the 64 protozoan taxa recorded during EIFEX, 22 were identified to species and 42 to genus level. Figure 1 shows total integrated protozooplankton standing stocks for the upper 100 m and for those stations where all taxa have been sampled. Inside the patch, protozooplankton standing stocks increased from 1.0 to 1.3 g C m^{-2} by day 28, and declined to initial values thereafter (Fig. 1A). Standing stocks outside the patch remained remarkably constant at 0.7 ± 0.04 g C m^{-2} (Fig. 1B). While total standing stocks varied little both inside and outside the patch, there was considerable turn-over within the species populations comprising the protozooplankton, reflected in shifts in the relative contribution of the major taxa over the course of the experiment (Fig. 1). HNF accounted for $2-5\%$ of protozooplankton standing stocks inside and outside the patch and showed no clear temporal trend. Aloricate ciliates were initially the largest component of protozooplankton standing stocks ($\sim 30\%$) but declined both inside and outside the patch. While contributing less biomass than aloricate ciliates, the contribution of tintinnid biomass increased from 3 to 12% of total protozooplankton stock inside the patch while staying at low levels outside. Similar diverging patterns could be observed for athecate and thecate dinoflagellates inside the patch; the relative contribution of the former declined from initially 29 to 9%, while the latter increased biomass from 8 to 13% by the end of the experiment. Outside the patch all dinoflagellates declined, in particular thecate dinoflagellates reached negligible levels at the end of the experiment. Acantharians
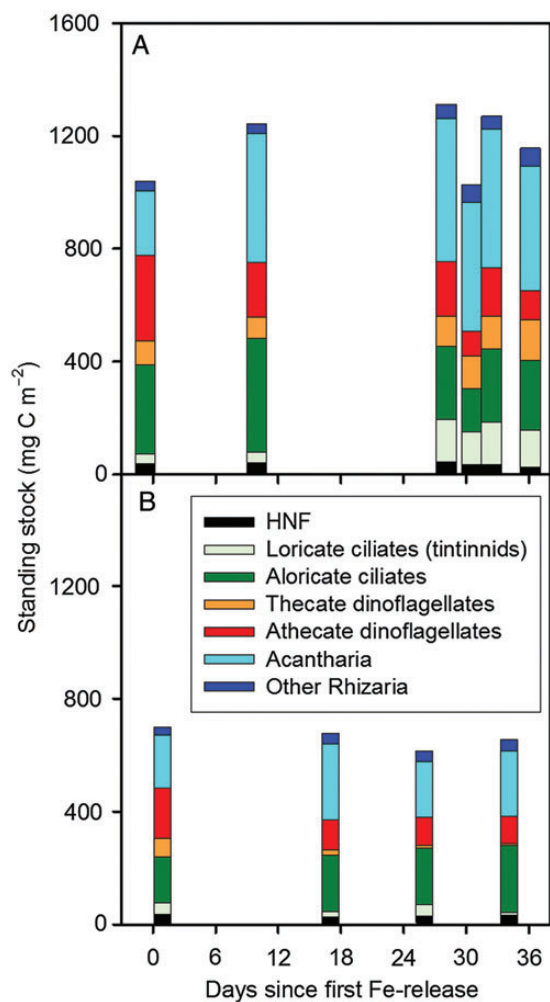
Fig. 1. Protozooplankton standing stocks integrated over the upper 100 m inside (**A**) and outside (**B**) the fertilized patch.

doubled their relative contribution from initially 22 to 44% inside the patch while remaining at constant levels outside the patch. Other rhizaria, including foraminifera, polycystines, phaeodaria and the taxopodidan *Sticholonche zanclea*, accounted for only a small fraction of the protozooplankton biomass (3−7%). Among these taxa foraminifera accounted for the largest share in biomass, while phaeodaria and *S. zanclea*, despite being minor constituents, increased their contribution to protozoan standing stocks inside the patch by three- and nine-fold, respectively.

Vertical distribution

The upper layer of the EIFEX eddy was characterized by warm and fresh Antarctic surface water (ASW). Below the ASW and the relatively warm upper circumpolar deep water lies a temperature minimum layer between 200 and 300 m, which is generally considered the remnant of the previous winter mixed layer, and is thus known as winter water (WW) (Park *et al.*, 1998). According to the temperature minimum criterion, the lower boundary of the winter mixed layer was situated at around 250 m inside and between 200 and 250 m depth outside the patch (upper panels in Fig. 2; see also Hibbert *et al.*, 2009). For this study, the mixed layer depth was defined, as in Cisewski *et al.* (Cisewski *et al.*, 2005), by the depth at which the calculated *in situ* density increased by $\Delta\sigma_T = 0.02$ kg m^{-3} compared with the surface value and was around 100 m throughout EIFEX both inside and outside the patch (upper panels in Fig. 2; see also Cisewski *et al.*, 2008).

The different protozooplankton taxa showed distinct vertical distribution patterns. Acantharians peaked and declined in the surface-mixed layer inside the patch, with very low concentrations below 150 m depth. Patterns of vertical distribution were similar outside the patch but biomass declined during the experiment (Fig. 2). Pronounced surface maxima were observed for all acantharian genera differentiated during this study. Inside the patch, pallium-feeding thecate dinoflagellates, represented by *Protoperidinium* spp. and *Diplopsalis* spp., were initially distributed down to 250 m depth while during the latter half of the experiment peak abundances were restricted to the upper 100 m of the water column (Fig. 2). Outside the fertilized patch, pallium-feeding dinoflagellates were more abundant below the mixed layer with the exception of the first out-patch station (Fig. 2). Inside the patch, tintinnid abundance showed a marked increase in the upper 100 m of the water column and sharply declined below 150 m (Fig. 2). Tintinnid abundance outside the patch peaked close to the bottom of the mixed layer between 80 and 100 m but declined towards the end of the experiment (Fig. 2). Foraminifera showed peak abundances within the surface-mixed layer and down to 200 m depth both inside and outside the patch (Fig. 2). Inside the patch, abundance of *Sticholonche zanclea* peaked both within and below the surface-mixed layer down to depths of 150 m, while it peaked at the bottom of the mixed layer between 80 and 150 m depth outside the patch (Fig. 2). Abundances of peduncle-feeding thecate dinoflagellates, represented by *Dinophysis* spp. and *Phalacroma* spp., showed distinct deep maxima at 200 − 250 m depth and 150 − 250 m depth inside and outside the patch, respectively (Fig. 2). Phaeodarian abundances peaked between 150 and 250 m depth both inside and outside the patch (Fig. 2). These deep-dwelling taxa were notably absent or rare in the surface-mixed layer and exhibited abundance maxima associated with WW.
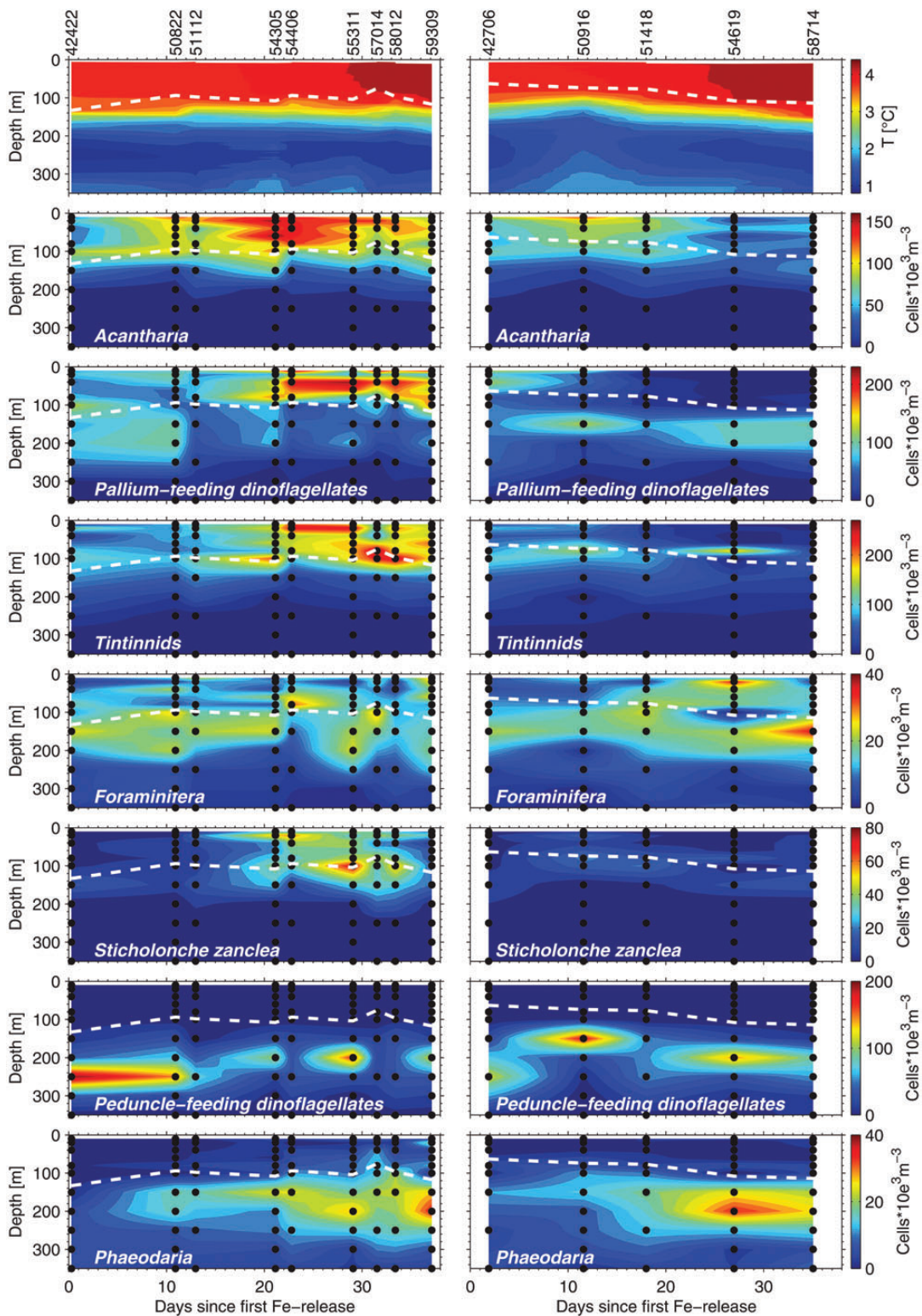
Fig. 2. Vertical distribution of acantharia, pallium-feeding dinoflagellates, tintinnids, foraminifera, *Sticholonche zanclea*, peduncle-feeding dinoflagellates and phaeodaria inside (left column) and outside (right column) the fertilized patch. The uppermost panels depict the temperature distribution inside and outside the patch, respectively; the mixed layer depth is indicated by the dashed white line. The sampling depths are indicated with a black dot.

Distribution of tintinnid loricae along the deep water column

Full tintinnid loricae accounted for only a minor fraction of total loricae below 500 m depth, while intact empty and damaged loricae were found throughout the deep water column both underneath the fertilized patch and outside of it (Fig. 3). Stocks of empty and damaged loricae were generally higher underneath the patch than outside it and at the edge-patch station. A marked increase of empty and damaged tintinnid loricae was observed in the nepheloid layer (the lowermost layer) at the in-patch station on day 36.
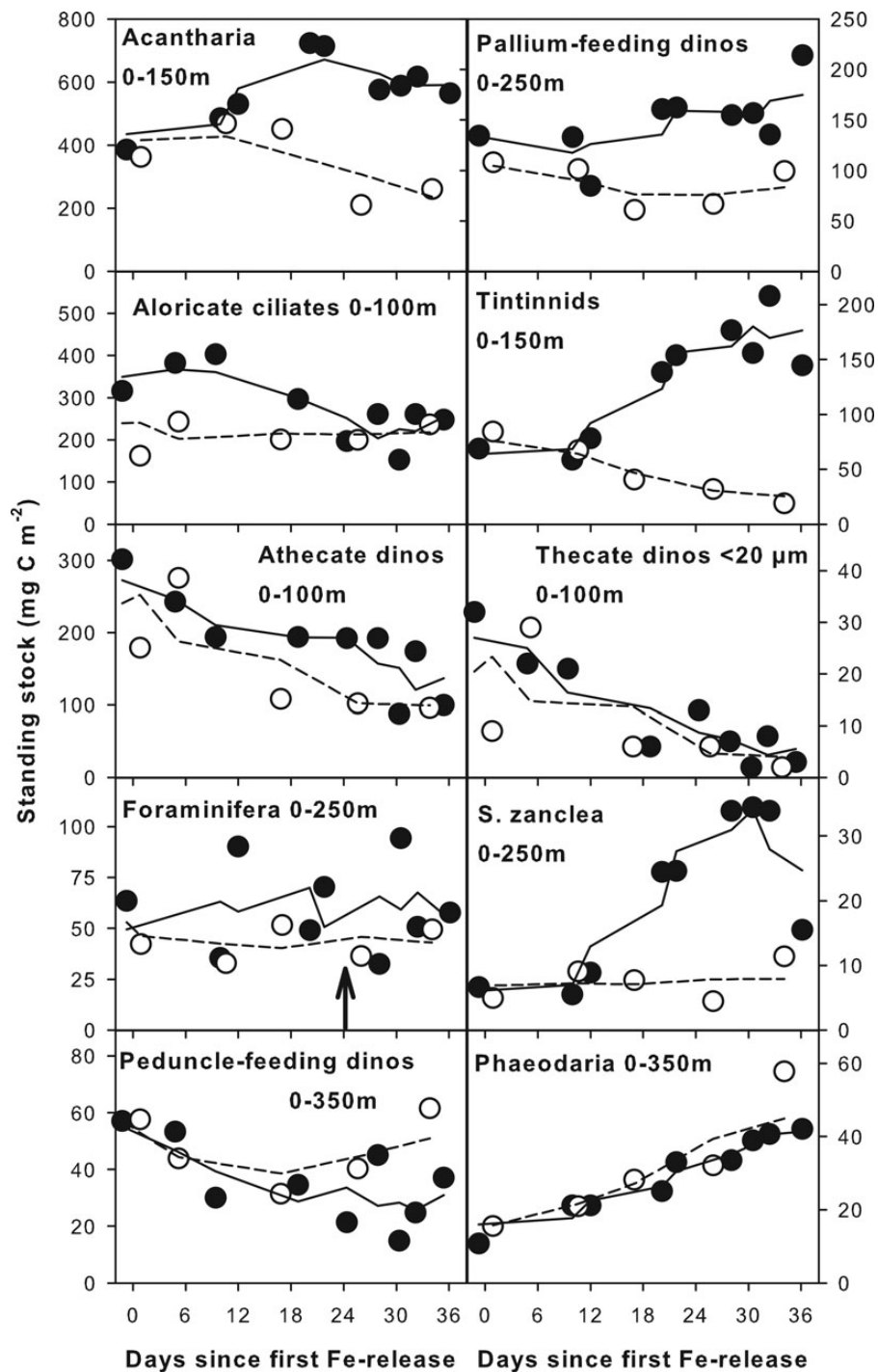
Temporal trends inside and outside the patch

Standing stocks of the dominant protozooplankton taxa were integrated over the upper 100 to 350 m according to their vertical distribution patterns. Acantharian standing stocks increased linearly at a rate of 0.03 day^{-1} inside the patch until day 20 and declined thereafter while outside the patch, stocks remained relatively stable (Fig. 4). The slope of the in-patch linear regression line for the increase until day 20 was significantly different from the outside slope (b_In = 5.06, b_Out = −5.59, $P = 0.043$; where the P-value correspond to the null hypothesis H0 'equal slopes' for the in-patch and out-patch trends in standing stocks). Two genera, *Acanthostaurus* spp. and *Gigartacon* spp., dominated acantharian standing stocks while the remaining genera had a relatively minor contribution (Supplementary data, Fig. S2). Stocks of pallium-feeding dinoflagellates accumulated only slightly at 0.01 day^{-1} inside the patch while staying relatively stable outside the patch (Fig. 4). There was no significant difference between the linear slopes inside and outside the patch (b_In = 1.72, b_Out = −0.595, $P = 0.11$). Inside the patch, standing stocks of aloricate ciliates showed an initial increase to 0.4 g C m^{-2} on day 12 and declined thereafter, while stocks stayed relatively constant outside the patch (Fig. 4). The slope of the in-patch linear regression was significantly different from the outside slope (b_In = −4.52, b_Out = 0.971, $P = 0.043$). *Strombidium* spp. and *Strobilidium* spp. together accounted for the
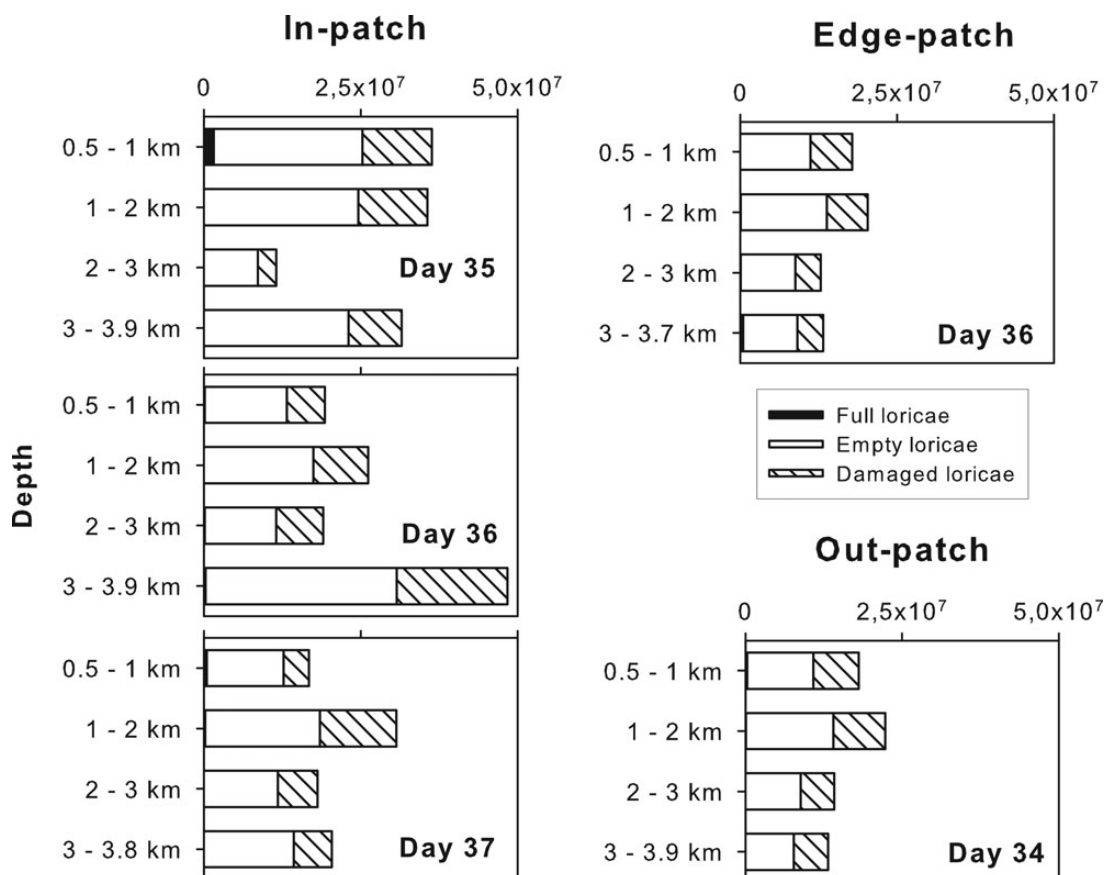
Fig. 3. Integrated abundances (in loricae m^{-2}) of full, empty and damaged tintinnid loricae in four depth bins from 500 m depth to the sea floor for three in-patch stations (days 35, 36 and 37), one edge-patch station (day 36) and one out-patch station (day 34).

Fig. 4. Temporal trends in integrated standing stocks of the dominant protozooplankton taxa inside (filled black circles) and outside (open black circles) the fertilized patch. The lines represent the running averages over three temporally adjacent in-patch (solid line) and out-patch (dashed line) stations, respectively. The black arrow in panel G indicates the full-moon event. Integration depths for the different taxa are indicated in their respective panels and were chosen according to their depth distribution.

largest share of aloricate ciliate standing stocks (Supplementary data, Fig. S3). Stocks of *Strobilidium* spp. and of the third most important genus *Tontonia* declined both inside and outside the patch while those of

Strombidium spp., although variable, remained more stable (Supplementary data, Fig. S3). Inside the patch, stocks of tintinnids increased three-fold from day 10 until day 28 at a rate of $0.06 \, \mathrm{day}^{-1}$, while stocks outside the patch

declined (Fig. 4). The slopes of the linear regressions were significantly different between inside and outside the patch (b_In = 3.64, b_Out = −2.02, P = 0.00067). Agglutinated tintinnids (*Codonellopsis pusilla, C. gausii* and *Stenosemella* spp.) dominated numerically, while the large-sized, hyaline species *Cymatocylis calyciformis, C. vanhoeffeni* and *C. nobilis* combined dominated in terms of biomass (Supplementary data, Fig. S4). Interestingly, *C. calyciformis* declined over the course of the experiment, while *C. vanhoeffeni* and *C. nobilis* increased (Supplementary data, Fig. S4). Among the agglutinated genera, *Stenosemella* spp. showed the strongest increase inside the patch (Supplementary data, Fig. S4). Both athecate and thecate dinoflagellates < 20 µm showed a similar decline inside and outside the patch (Fig. 4), supported by non-significant differences in the slopes different between inside and outside (b_In = −4.26, b_Out = −4.31, P = 0.98 in case of athecate dinoflagellates; b_In = −0.725, b_Out = −0.495, P = 0.44 in case of thecate dinoflagellates <20 µm). Athecate dinoflagellates mostly comprised members of the genera *Amphidinium*, *Gymnodinium* and *Gyrodinium* at strikingly equal proportions during the first half of the experiment both inside and outside the patch (Supplementary data, Fig. S5). Thecate dinoflagellates <20 µm were largely composed of unidentified thecate taxa, while peridinoids and *Oxytoxum* spp. accounted for only a minor share of standing stocks (Supplementary data, Fig. S6). Among the large (>20 µm) thecate dinoflagellates, *Protoperidinium* spp. dominated standing stocks, followed by *Dinophysis* spp. and *Diplopsalis* spp. (Supplementary data, Fig. S7). Foraminifera were characterized by oscillating standing stocks both inside and outside the patch (Fig. 4) and showed no significant differences between inside and outside trends (b_In = −0.0584, b_Out = 0.194, P = 0.8). Adult foraminifera clearly dominated over juveniles and accounted for 71 to 94% of total foraminiferan biomass inside and outside the patch. The spinose species *Globigerina bulloides* followed by *Turborotalita quinqueloba* dominated in terms of abundance and biomass inside the patch, while stocks of the non-spinose *Neoglobigerina pachyderma* were similar to those of *G. bulloides* outside the patch (Supplementary data, Fig. S8). Stocks of the taxopodidan *Sticholonche zanclea* quadrupled from days 12 to 32 at a rate of 0.11 day^{-1} inside the patch and declined thereafter (Fig. 4). Standing stocks outside the patch stayed remarkably constant. The slope of the in-patch linear regression until day 32 was significantly different from the out-patch slope (b_In = 1.05, b_Out = 0.105, P = 0.0012).

Among the deep-dwelling taxa, nassellarians and spumellarians were a negligible contribution to protozooplankton standing stocks. *Antarctissa* spp. dominated nassellarian, while *Spongotrochus glacialis* dominated spumellarian standing stocks (Supplementary data, Figs S9 and S10). Inside the patch stocks of peduncle-feeding dinoflagellates initially declined but stabilized thereafter while being more stable outside the patch (Fig. 4). No significant differences between inside and outside trends were observed (b_In = −0.725, b_Out = 0.0551, P = 0.24). Phaeodarian stocks showed a constant linear increase at a rate of 0.08 day^{-1} both inside and outside the patch (Fig. 4). The increasing trends both inside and outside were not significantly different from each other (b_In = 0.863, b_Out = 1.17, P = 0.18). *Protocystis* spp. dominated phaeodarian abundance and biomass both inside and outside the patch followed by species of the genus *Challengeria* (Supplementary data, Fig. S11). Species of the former genus were almost exclusively responsible for the linear increase inside and outside the patch (Supplementary data, Fig. S11).
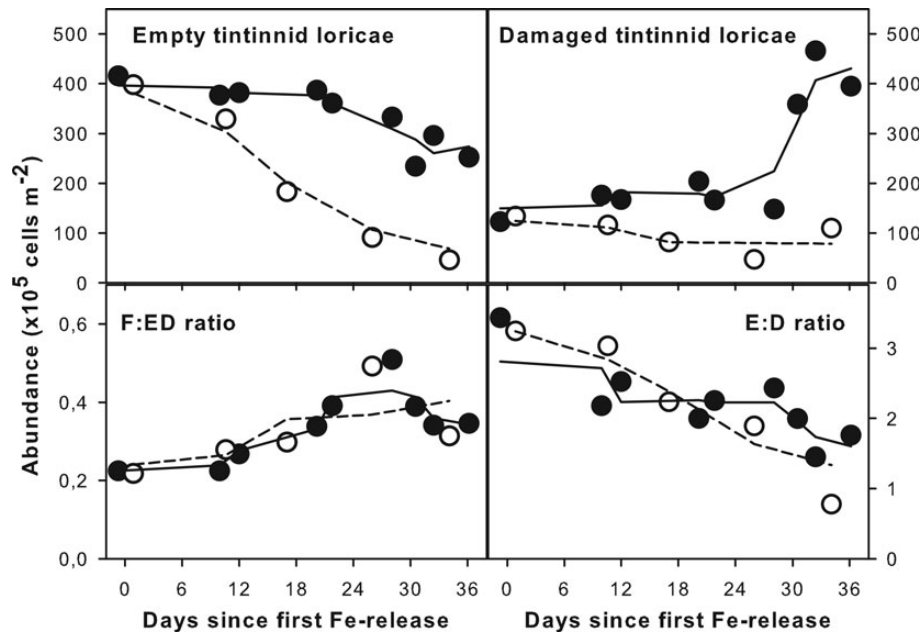
Temporal trends of empty and damaged tintinnid loricae

Intact empty tintinnid loricae declined both inside and outside the fertilized patch albeit at a steeper rate outside (Fig. 5) which is reflected in significant differences in the slopes (b_In = −4.55, b_Out = −11.4, P = 0.0021). Damaged loricae changed little in fertilized waters until day 30 but dramatically increased thereafter, while they slightly declined outside the patch (Fig. 5). The in-patch and out-patch slopes for damaged loricae were significantly different from each other (b_In = 7.89, b_Out = −1.41, P = 0.03). The ratio of full to empty and damaged loricae (F:ED) was always well below one and remarkably similar inside and outside the fertilized patch (Fig. 5). The ratio of intact empty to damaged loricae (E:D) declined continuously inside and outside the patch, albeit at a steeper rate outside the patch (Fig. 5).

DISCUSSION

Ecological conditions during the experiment

The water of the eddy core originated, from the Antarctic Zone (AZ), the southernmost belt of the permanently ice-free ACC indicated by high late-summer silicate concentrations of 19 mmol m^{-3} and the characteristic large, heavily silicified diatom species (Assmy *et al.*, 2013). The region was clearly iron-limited and phytoplankton stocks in unfertilized waters decreased by 40% over the 37 days. Iron addition led to an increase in photosynthetic efficiency (Fv/Fm ratios) which stayed at high levels (0.4−0.6) throughout (Berg *et al.*, 2011), indicating that

Fig. 5. Temporal trends in empty and damaged tintinnid loricae integrated over 350 m and ratios of full to empty and damaged loricae (F:ED) and empty to damaged loricae (E:D) inside (filled black circles) and outside (open black circles) the fertilized patch. The lines represent the running averages over three temporally adjacent in-patch (solid line) and out-patch (dashed line) stations, respectively.

the phytoplankton assemblage remained iron-replete until the end. Diatom stocks increased three-fold inside the patch during the first 3 weeks and contributed 97% of the total increase in phytoplankton biomass (Smetacek *et al.*, 2012). Of the diatom species that responded strongly to iron input, some underwent mass mortality, formed aggregates and sank out of the surface layer in the last 2 weeks (in particular *Chaetoceros* spp.), while the populations of others remained stable at high levels or continued to increase until the end of the experiment. The latter diatoms were exceptionally large, heavily silicified and had low mortality rates estimated from the ratios of living cells to empty and broken frustules (Assmy *et al.*, 2013). They will have been inaccessible to most protozoan grazers. In contrast, the biomass of total, non-diatom phytoplankton, dominated by nanoflagellates largely comprising solitary *Phaeocystis* cells, remained stable at low levels (0.8 ± 0.1 g C m^{-2}), although various other less-abundant species increased and declined during the course of the experiment. We attribute the lack of biomass build-up despite iron-enhanced growth rates of the nanoflagellates to grazing pressure of the protozooplankton, as biomass of salps, their other major grazers, was very low.

Metazooplankton was dominated by copepods that contributed between 30 and 40% of total plankton biomass (Assmy *et al.*, 2013). Copepod grazing pressure increased during the experiment both inside and outside the patch but was more intense inside. This was reflected

in the increase of copepod faecal pellets and copepod grazing rates in the surface-mixed layer (Assmy *et al.*, 2013) and in the triggering of egg production in *Rhincalanus gigas*, one of the dominant copepod species, by the EIFEX bloom (Jansen *et al.*, 2006). Since the bulk of total protistan biomass was present in grazer-protected diatoms, copepod grazing pressure will have been accordingly intense on the other protists, in particular the protozooplankton. Assmy *et al.* (Assmy *et al.*, 2013) present evidence for species-specific selective grazing on diatoms by copepods based on the ratios living (full cells) to empty intact and broken diatom frustules. They argue, using tintinnid loricae as an example, that grazer control by copepods on the populations of protozooplankton was much more intense than on the diatoms. Dilution experiments conducted during EIFEX also showed a progressive decoupling between microzooplankton grazing rates, largely ciliates and dinoflagellates, and diatom growth rates which was mainly attributed to top-down control of the former by copepods (Latasa *et al.*, in press). This type of trophic cascade has been reported from many regions (e.g. Froneman and Bernard, 2004) and has been proposed as a precondition for development of phytoplankton blooms (Irigoien *et al.*, 2005; Sherr and Sherr, 2009).

The bulk of protozooplankton biomass ($>90\%$) was present in the three groups Acantharia, dinoflagellates and ciliates. The species that accumulated biomass in each of these groups, in analogy to the higher

accumulation rates of the grazer-protected diatom species, were at the upper end of the respective group size ranges and were protected by thick, outward-pointing spines of strontium sulphate (Acantharia), stiff, durable, proteinacous shells (tintinnid loricae) or thick cellulose plates (armoured dinoflagellates). In contrast, the smaller, less protected representatives of the ciliates and dinoflagellates declined in the course of the experiment, as also in outside water. Ciliates are known as specialized grazers of nanoflagellates, hence the low, albeit steady biomass levels of both auto- and heterotrophic fractions of the latter can well have been maintained by the ciliates. In the case of HNF, food supply is not likely to have been limiting as the biomass of their main prey, bacteria, was in the same range as that of total protozooplankton and bacterial production rates accounted for a substantial portion (about one quarter) of total primary production (Assmy *et al.*, 2013). In the following, we present the case for top-down vs. bottom-up control of stocks of the various protozooplankton groups.

Ciliates

During the first Subarctic Pacific Iron *Experiment* for Ecosystem Dynamics Study (SEEDS I), biomass standing stocks of aloricate ciliates were remarkably similar to those recorded in EIFEX, both inside and outside the patch, while tintinnid stocks were considerably lower (Saito *et al.*, 2005). During the Kerguelen Ocean and Plateau compared Study (KEOPS) on the other hand, tintinnid stocks inside the bloom area were similar to peak tintinnid stocks recorded at the end of EIFEX, while aloricate stocks were considerably lower than during EIFEX (Christaki *et al.*, 2008). During the Southern Ocean iron release experiment (SOIREE), ciliates accounted for only a minor fraction $(3-10\%)$ of protozooplankton biomass, while HNF dominated (Hall and Safi, 2001). These differences in total biomass and relative proportions of the protozooplankton assemblages from different sites and seasons suggest corresponding differences in their impact on their prey organisms, from bacteria to diatoms.

Large species of the tintinnid genus *Cymatocylis* are particularly common in the Southern Ocean (Dolan *et al.*, 2012) and dominated biomass of tintinnids as was also reported from EisenEx and KEOPS (Christaki *et al.*, 2008; Henjes *et al.*, 2007). The species replacement we observed, a decline in *C. calicyformis* and an increase in *C. vanhoeffeni* and *C. nobilis* of similar size and shape, is a previously described feature of tintinnid ecology (Dolan *et al.*, 2013). As mentioned above, copepod grazing pressure on tintinnids was much higher than that on diatoms. The ratios of living cells at the time of sampling to empty

and damaged frustules and loricae in total diatom and tintinnid species, respectively, was always above 3 in diatoms and below 0.6 in tintinnids. Apart from natural mortality, empty, intact loricae can also be attributed to an artefact of handling during the sampling procedure. Based on the absence of a significant difference in these ratios in results from different sampling techniques, this effect was discounted by Henjes *et al.* (Henjes *et al.*, 2007). Damaged loricae on the other hand can only be due to crustacean gnathosomes (copepods) or gastric mills (euphausiids). The rapid increase in damaged tintinnid loricae toward the end of EIFEX closely matched the concomitant increase in integrated copepod fecal pellet standing stocks inside the patch (Assmy *et al.*, 2013). Besides, damaged loricae, but also intact ones, were frequently found within copepod fecal pellets.

The elevated values of empty and damaged tintinnids in the deep water column and their increase in the nepheloid layer below the fertilized patch are remarkable and suggest that tintinnid loricae contribute to deep vertical carbon flux, whereas the other protozoan groups were largely dissolved within the upper 1000 m. Fecal pellets were the main source of damaged loricae, but most pellets were retained within the surface-mixed layer, while stocks of empty and damaged loricae were similar in surface and subsurface layers (Assmy *et al.*, 2013) presumably because of the greater durability of the proteinaceous (Agatha and Simon, 2012), stiff and leathery loricae once released from degraded fecal pellets. Although empty and damaged loricae were present both underneath the patch and outside it, increased copepod grazing pressure inside the patch might have contributed to their elevated stocks in the deep water column underneath the patch. Since the lorica can account for up to 60% of tintinnid carbon content (Gilron and Lynn, 1989), the export of empty and damaged tintinnid loricae below the surface-mixed layer indicates that they can be an important component of the biological carbon pump. Assuming the above factor, integrated stocks of full, empty and damaged tintinnids for the entire water column below 100 m accounted for 0.3 g C m^{-2} at the deep out-patch station and up to 0.6 g C m^{-2} at the deep in-patch station on day 36. The in-patch estimate on day 36 corresponds to 10% of the background vertical export from the hot spot of the fertilized patch extrapolated for the entire duration of the experiment (Smetacek *et al.*, 2012).

Dinoflagellates

The marked decline in athecate dinoflagellates contrasts with their pronounced increase, in particular *Gyrodinium* spp., during the SEEDS I experiment (Saito *et al.*, 2005).

This marked increase was attributed to the ability of *Gyrodinium* species to feed on the chain-forming *Chaetoceros debilis* (Saito *et al.*, 2006) which accounted for the bulk of bloom biomass (Tsuda *et al.*, 2003). Although small, solitary pennate diatoms, e.g. *Thalassionema nitzschioides*, were occasionally found engulfed by gymnodinoids, grazing of athecate dinoflagellates on the chain-forming and spiny diatoms dominating the EIFEX bloom was not observed. During EIFEX, the combination of dominance of large, well-protected diatoms and heavy copepod grazing was likely responsible for the decline in athecate dinoflagellates, as in the case of aloricate ciliates. The same applies to thecate dinoflagellates <20 μm, which were recorded at very low abundances inside and outside the patch by the end of the experiment. Although little is known about the feeding habits of the small peridinoids and *Oxytoxum* species (Jacobson, 1999), it is likely that they were not capable of feeding on the large diatoms responsible for the iron-induced bloom. In contrast, large pallium-feeding dinoflagellates capable of feeding on large diatoms (Jacobson, 1999; Jacobson and Anderson, 1986) shifted their maxima from subsurface to surface layers within the patch but declined or descended to greater depths outside the patch. Whether this was due to vertical migration or the effect of local mortality and growth is unknown. In any case, this group was clearly stimulated by the diatom bloom. The distinct deep maxima observed in the peduncle-feeding dinoflagellates *Dinophysis* and *Phalacroma* corresponded to the depth range of the winter mixed layer and possibly represent stages in quiescent mode (Reguera *et al.*, 2012).

Rhizaria

The larger contribution of acantharian biomass than either ciliates or dinoflagellates to total protozooplankton biomass is noteworthy but not necessarily unusual as acantharia spines dissolve in samples not amended with excess strontium and hence the group tends to be overlooked. Similar biomass levels were also found in spring during EisenEx (Henjes *et al.*, 2007). Low mortality rates are indicated by the low incidence of these conspicuous organisms in copepod guts (Kruse *et al.*, 2009) and the low percentage of skeletons without plasma (<10%) to intact organisms in water samples. Apparently, the numerous outward-pointing, sharp spines characteristic of acantharians afford protection against grazing. Despite their low mortality acantharian biomass only doubled in the first 3 weeks suggesting that their growth rates are lower than those of ciliates and dinoflagellates. Acantharians feed on a large variety of food items ranging from bacteria to copepod nauplii and in particular motile protozoa (Caron and Swanberg, 1990).

Some acantharian species are known to host autotrophic symbionts (Michaels, 1988), so confinement to the surface-mixed layer is advantageous in terms of access to light. A recent study of the molecular phylogeny and morphological evolution of acantharians has identified six major clades within this group (Decelle *et al.*, 2012). Two out of the six clades (clades E and F) include species that host symbiotic algae in their cytoplasm, do not form cysts and complete their entire life cycle in the euphotic zone, while cyst-forming acantharians belonging to clades A–C spend part of their life cycle in the deep ocean via their sinking cysts and are generally not associated with symbionts (Decelle *et al.*, 2013). *Acanthostaurus* belongs to the symbiotic acantharia within clade F, while *Gigartacon* comprises cyst-forming acantharians which scatter over various sub-clades within clade C (Decelle *et al.*, 2012). Although acantharians of clade C generally do not harbour symbionts, there are exceptions to this rule (Decelle *et al.*, 2012), which apparently also applied to the *Gigartacon* species encountered during EIFEX, where specimens with endosymbionts have often been observed. Possibly, the positive response to iron addition could have been due to stimulation of endosymbiont growth. Despite their extremely high ballast conferred by the heavy mineral spines (celestite is by far the heaviest biogenic mineral) and their large biomass, acantharian contribution to vertical carbon flux is probably restricted to the upper 250 m as these organisms and their remains were only found at very low abundances below that depth. It is worth pointing out here that the mechanism counteracting the weight of the spines and enabling maintenance in the surface layer is unknown (Smetacek, 2012).

Foraminifera have complex reproductive behaviour; hence the lack of a clear response to the bloom is not surprising. Previous observations have shown a synodic lunar periodicity in the reproductive cycle of foraminifera species (Bijma *et al.*, 1990; Hemleben *et al.*, 1989; Spindler *et al.*, 1979), including EisenEx (Henjes *et al.*, 2007), but we observed neither an increase in juvenile nor adult foraminifera subsequent to the full-moon event falling within the time frame of EIFEX.

Although a minor contributor to protozooplankton standing stocks, *Sticholonche zanclea*, showed the most pronounced increase of all protozoans inside the patch, with accumulation rates rivalling those of the dominant diatom species during EIFEX (Assmy *et al.*, 2013) and exceeding those of all other protozoan taxa. This contrasts with the lack of a clear response during EisenEx (Henjes *et al.*, 2007), where abundances inside and outside the fertilized patch remained similar. *Sticholonche zanclea* showed a deeper distribution than acantharians, with slightly deeper maxima outside than inside the patch. Similar vertical

distribution patterns were observed during a study from the equatorial Pacific (Takahashi and Ling, 1980). Since little is known about the ecology of *S. zanclea,* its food preferences can be inferred from those of its close relatives the acantharians or the planktonic heliozoan *Actinophrys sol.* Both have been reported to feed mostly on motile protozoa, in particular ciliates (Caron and Swanberg, 1990; Pierce and Coats, 1999; Trégouboff, 1957). Thus, *S. zanclea* might have profited from increasing tintinnid stocks inside the patch. The lack of a response of *S. zanclea* during EisenEx could thus be explained by the concomitant low and more or less constant tintinnid standing stocks (Henjes *et al.,* 2007). Capture of motile prey organisms is apparently enabled by the axopodia, which are used by *S. zanclea* as oars to propel itself through seawater (Cachon *et al.,* 1977). The limited number of studies dealing with the distribution and ecology of *Sticholonche* (Gowing, 1989; Gowing and Garrison, 1991, 1992; Henjes *et al.,* 2007; Klaas, 2001) warrant further research on the ecology of this enigmatic species.

Distinct subsurface maxima similar to those observed during EIFEX were reported during a previous study investigating Southern Ocean phaeodarian assemblages (Abelmann and Gowing, 1996). Phaeodarians are known mesopelagic flux feeders intercepting particles emanating from surface layer. The similar linear trends in phaeodarian standing stocks inside and outside the patch suggests that they were feeding on the continuous background flux measured underneath the patch and outside of it but did not respond to the massive export event triggered by the collapse of the iron-induced bloom (Smetacek *et al.,* 2012). The food vacuole of phaeodarians, the phaeodium (Caron and Swanberg, 1990), was frequently observed to contain diatom fragments and other remnants of planktonic origin supporting the observation that they feed on detritus and sinking organic aggregates originating from the productive surface layer (Gowing and Bentham, 1994; Nöthig and Gowing, 1991). Maximum phaeodarian stocks seem to coincide with the summer season when mesopelagic biomass is at its highest (Abelmann and Nimmergut, 2005).

CONCLUSIONS

Total protozooplankton biomass was constrained by selective grazing of the large copepod stock enabling large, spiny, heavily silicified diatoms to dominate bloom biomass.

Acantharia can be as important as ciliates and dinoflagellates in their contribution to total protozooplankton biomass but have been overlooked in the past because their prominent spines dissolve in sea water samples not amended with strontium chloride. We strongly recommend this procedure for future studies of pelagic ecosystems as little is known about their biology and effect on vertical flux.

It is likely that the bulk of tintinnid loricae, although proteinaceous, are not digested by copepods nor respired in the water column like chitin exoskeletons, hence reach abyssal depths. Given the ubiquity of tintinnids in the sea, their loricae are likely to play a relevant role in the biological carbon pump.

The linear, increasing trend of phaeodarian biomass in the subsurface layer, remarkably similar both inside and outside the patch, implies the presence of a seasonal cycle in their life histories not affected by mass-sinking, post-bloom events. This observation might be of significance given their proxy role in paleoceanography.

The high accumulation rates of the little known *Sticholonche zanclea* are an indication of the growth potential of protozooplankton.

SUPPLEMENTARY DATA

Supplementary data can be found online at http://plankt.oxfordjournals.org.

REFERENCES

Abelmann, A. and Gowing, M. M. (1996) Horizontal and vertical distribution pattern of living radiolarians along a transect from the Southern Ocean to the South Atlantic subtropical region. *Deep-Sea Res. Pt. I,* **43**, 361–382.

Abelmann, A. and Gowing, M. M. (1997) Spatial distribution pattern of living polycystine radiolarian taxa—baseline study for paleoenvironmental reconstructions in the Southern Ocean (Atlantic sector). *Mar. Micropaleontol.,* **30**, 3–28.

Abelmann, A. and Nimmergut, A. (2005) Radiolarians in the Sea of Okhotsk and their ecological implication for paleoenvironmental reconstructions. *Deep-Sea Res. Pt. II*, **52**, 2302–2331.

Adl, S. M., Simpson, A. G. B., Lane, C. E. *et al.* (2012) The revised classification of eukaryotes. *J. Eukaryot. Microbiol.*, **59**, 429–493.

Agatha, S. and Simon, P. (2012) On the nature of tintinnid loricae (Ciliophora: Spirotricha: Tintinnina): a histochemical, enzymatic, EDX, and high-resolution TEM study. *Acta Protozool.*, **51**, 1–19.

Assmy, P., Smetacek, V., Montresor, M. *et al.* (2013) Thick-shelled, grazer-protected diatoms decouple ocean carbon and silicon cycles in the iron-limited Antarctic Circumpolar Current. *Proc. Natl Acad. Sci. USA*, **110**, 20633–20638.

Bé, A. W. H., Hemleben, C., Anderson, O. R. *et al.* (1977) Laboratory and field observations of living planktonic foraminifera. *J. Micropaleontol.*, **23**, 155–179.

Berg, G. M., Mills, M. M., Long, M. C. *et al.* (2011) Variation in particulate C and N isotope composition following iron fertilization in two successive phytoplankton communities in the Southern Ocean. *Global Biogeochem. Cycles*, **25**, Gb3013.

Bijma, J., Erez, J. and Hemleben, C. (1990) Lunar and semi-lunar reproductive cycles in some spinose planktonic foraminifers. *J. Foramin. Res.*, **20**, 117–127.

Boyd, P. W., Jickells, T., Law, C. S. *et al.* (2007) Mesoscale iron enrichment experiments 1993–2005: synthesis and future directions. *Science*, **315**, 612–617.

Cachon, J., Cachon, M., Tilney, L. G. *et al.* (1977) Movement generated by interactions between the dense material at the ends of microtubules and non-actin-containing microfilaments in Sticholonche zanclea. *J. Cell Biol.*, **72**, 314–338.

Calbet, A. and Saiz, E. (2005) The ciliate-copepod link in marine ecosystems. *Aquat. Microb. Ecol.*, **38**, 157–167.

Caron, D. A., Countway, P. D., Jones, A. C. *et al.* (2012) Marine protistan diversity. In Carlson, C. A. and Giovannoni, S. J. (eds), Annual Review of Marine Science, *Vol.* 4. Annual Reviews, Palo Alto, USA, pp. 467–493.

Caron, D. A. and Swanberg, N. R. (1990) The ecology of planktonic sarcodines. *Rev. Aquat. Sci.*, **3**, 147–180.

Chow, C. -E. T., Kim, D. Y., Sachdeva, R. *et al.* (2013) Top-down controls on bacterial community structure: microbial network analysis of bacteria, T4-like viruses and protists. *ISME J.*, **7**, 1–14.

Christaki, U., Obernosterer, I., Van Wambeke, F. *et al.* (2008) Microbial food web structure in a naturally iron-fertilized area in the Southern Ocean (Kerguelen Plateau). *Deep-Sea Res. Pt. II*, **55**, 706–719.

Cisewski, B., Strass, V. H., Losch, M. *et al.* (2008) Mixed layer analysis of a mesoscale eddy in the Antarctic Polar Front Zone. *J. Geophys. Res.-Oceans*, **113**, C05017.

Cisewski, B., Strass, V. H. and Prandke, H. (2005) Upper-ocean vertical mixing in the Antarctic Polar Front Zone. *Deep-Sea Res. Pt. II*, **52**, 1087–1108.

Decelle, J., Martin, P., Paborstava, K. *et al.* (2013) Diversity, ecology and biogeochemistry of cyst-forming Acantharia (Radiolaria) in the Oceans. *PLoS ONE*, **8**, e53598.

Decelle, J., Suzuki, N., Mahe, F. *et al.* (2012) Molecular phylogeny and morphological evolution of the Acantharia (Radiolaria). *Protist*, **163**, 435–450.

Dolan, J. R. (2010) Morphology and ecology in tintinnid ciliates of the marine plankton: correlates of lorica dimensions. *Acta Protozool.*, **49**, 235–244.

Dolan, J. R., Landry, M. R. and Ritchie, M. E. (2013) The species-rich assemblages of tintinnids (marine planktonic protists) are structured by mouth size. *ISME J.*, **7**, 1237–1243.

Dolan, J. R., Pierce, R. W., Yang, E. J. *et al.* (2012) Southern Ocean biogeography of tintinnid ciliates of the marine plankton. *J. Eukaryot. Microbiol.*, **59**, 511–519.

Fenchel, T. (1987) *Ecology of Protozoa: The Biology of Free-Living Phagotrophic Protists*. Madison Wisconsin, Science Tech Publishers.

Finlay, B. (2001) Protozoa. In: *Encyclopedia of Biodiversity*, Vol. 4. Academic Press, New York, pp. 901–915.

Froneman, P. W. and Bernard, K. S. (2004) Trophic cascading in the Polar Frontal Zone of the Southern Ocean during austral autumn 2002. *Polar Biol.*, **27**, 112–118.

Gilron, G. and Lynn, D. (1989) Assuming a 50% cell occupancy of the lorica overestimates tintinnine ciliate biomass. *Mar. Biol.*, **103**, 413–416.

Gowing, M. M. (1989) Abundance and feeding ecology of Antarctic phaeodarian radiolarians. *Mar. Biol.*, **103**, 107–118.

Gowing, M. M. and Bentham, W. N. (1994) Feeding ecology of phaeodarian radiolarians at the VERTEX North Pacific time series site. *J. Plankton Res.*, **16**, 707–719.

Gowing, M. M. and Garrison, D. L. (1991) Austral winter distributions of large tintinnid and large sarcodinid protozooplankton in the ice-edge zone of the Weddell/Scotia Seas. *J. Mar. Syst.*, **2**, 131–141.

Gowing, M. M. and Garrison, D. L. (1992) Abundance and feeding ecology of larger protozooplankton in the ice edge zone of the Weddell and Scotia Seas during the austral winter. *Deep-Sea Res. Pt. I*, **39**, 893–919.

Hall, J. A. and Safi, K. (2001) The impact of *in situ* Fe fertilisation on the microbial food web in the Southern Ocean. *Deep-Sea Res. Pt. II*, **48**, 2591–2613.

Hansen, B. W. and Jensen, F. (2000) Specific growth rates of protozooplankton in the marginal ice zone of the central Barents Sea during spring. *J. Mar. Biol. Assoc. UK*, **80**, 37–44.

Hemleben, C., Spindler, M. and Anderson, O. R. (eds) (1989) *Modern Planktonic Foraminifera*. Springer, New York.

Henjes, J. and Assmy, P. (2008) Particle availability controls agglutination in pelagic tintinnids in the Southern Ocean. *Protist*, **159**, 239–250.

Henjes, J., Assmy, P., Klaas, C. *et al.* (2007) Response of the larger protozooplankton to an iron-induced phytoplankton bloom in the Polar Frontal Zone of the Southern Ocean (EisenEx). *Deep-Sea Res. Pt. I*, **54**, 774–791.

Hibbert, A., Leach, H., Strass, V. H. *et al.* (2009) Mixing in cyclonic eddies in the Antarctic Circumpolar Current. *J. Mar. Res.*, **67**, 1–23.

Irigoien, X., Flynn, K. J. and Harris, R. P. (2005) Phytoplankton blooms: a 'loophole' in microzooplankton grazing impact?. *J. Plankton Res.*, **27**, 313–321.

Jacobson, D. M. (1999) A brief history of dinoflagellate feeding research. *J. Eukaryot. Microbiol.*, **46**, 376–381.

Jacobson, D. M. and Anderson, D. M. (1986) Thecate heterotrophic dinoflagellates: feeding behavior and mechanisms. *J. Phycol.*, **22**, 249–258.

Jansen, S., Klaas, C., Kragefsky, S. *et al.* (2006) Reproductive response of the copepod *Rhincalanus gigas* to an iron-induced phytoplankton bloom in the Southern Ocean. *Polar Biol.*, **29**, 1039–1044.

Katz, M. E., Cramer, B. S., Franzese, A. *et al.* (2010) Traditional and emerging proxies in foraminifera. *J. Foramin. Res.*, **40**, 165–192.

Klaas, C. (2001) Spring distribution of larger (>64 μm) protozoans in the Atlantic sector of the Southern Ocean. *Deep-Sea Res. Pt. I*, **48**, 1627–1649.

Krabberød, A. K., Brate, J., Dolven, J. K. *et al.* (2011) Radiolaria divided into Polycystina and Spasmaria in combined 18S and 28S rDNA phylogeny. *PLoS ONE*, **6**, e23526.

Kruse, S., Jansen, S., Krägefsky, S. *et al.* (2009) Gut content analyses of three dominant Antarctic copepod species during an induced phytoplankton bloom EIFEX (European iron fertilization experiment). *Mar. Ecol.*, **30**, 301–312.

Latasa, M., Henjes, J., Scharek, R. *et al.* (in press) Progressive decoupling between phytoplankton growth and microzooplankton grazing during an iron-induced phytoplankton bloom in the Southern Ocean (EIFEX). *Mar. Ecol. Prog. Ser.* doi: 10.3354/meps10937.

Menden-Deuer, S. and Lessard, E. J. (2000) Carbon to volume relationships for dinoflagellates, diatoms, and other protist plankton. *Limnol. Oceanogr.*, **45**, 569–579.

Michaels, A., Caron, D., Swanberg, N. *et al.* (1995) Planktonic sarcodines (Acantharia, Radiolaria, Foraminifera) in surface waters near Bermuda: abundance, biomass and vertical flux. *J. Plankton Res.*, **17**, 131–163.

Michaels, A. F. (1988) Vertical distribution and abundance of Acantharia and their symbionts. *Mar. Biol.*, **97**, 559–569.

Mutti, M. and Hallock, P. (2003) Carbonate systems along nutrient and temperature gradients: some sedimentological and geochemical constraints. *Int. J. Earth Sci.*, **92**, 465–475.

Nöthig, E.-M. and Gowing, M. M. (1991) Late winter abundance and distribution of phaeodarian radiolarians, other large protozooplankton and copepod nauplii in the Weddell Sea, Antarctica. *Mar. Biol.*, **111**, 473–484.

Park, Y.-H., Charriaud, E. and Fieux, M. (1998) Thermohaline structure of the Antarctic surface water/winter water in the Indian sector of the Southern Ocean. *J. Mar. Syst.*, **17**, 5–23.

Pernthaler, J. (2005) Predation on prokaryotes in the water column and its ecological implications. *Nat. Rev. Microbiol.*, **3**, 537–544.

Pierce, R. W. and Coats, D. W. (1999) The feeding ecology of *Actinophrys sol* (Sarcodina: Heliozoa) in Chesapeake Bay. *J. Eukaryot. Microbiol.*, **46**, 451–457.

Porter, K. G. and Feig, Y. S. (1980) The use of DAPI for identifying and counting aquatic microflora. *Limnol. Oceanogr.*, **25**, 943–948.

Reguera, B., Velo-Suarez, L., Raine, R. *et al.* (2012) Harmful *Dinophysis* species: a review. *Harmful Algae*, **14**, 87–106.

Rose, J. M. and Caron, D. A. (2007) Does low temperature constrain the growth rates of heterotrophic protists? Evidence and implications for algal blooms in cold waters. *Limnol. Oceanogr.*, **52**, 886–895.

Saito, H., Ota, T., Suzuki, K. *et al.* (2006) Role of heterotrophic dinoflagellate Gyrodinium sp in the fate of an iron induced diatom bloom. *Geophys. Res. Lett.*, **33**, L09602.

Saito, H., Suzuki, K., Hinuma, A. *et al.* (2005) Responses of microzooplankton to *in situ* iron fertilization in the western subarctic Pacific (SEEDS). *Prog. Oceanogr.*, **64**, 223–236.

Saiz, E. and Calbet, A. (2011) Copepod feeding in the ocean: scaling patterns, composition of their diet and the bias of estimates due to microzooplankton grazing during incubations. *Hydrobiologia*, **666**, 181–196.

Sarmiento, J. L., Gruber, N., Brzezinski, M. A. *et al.* (2004) High-latitude controls of thermocline nutrients and low latitude biological productivity. *Nature*, **427**, 56–60.

Sherr, E. B. and Sherr, B. F. (1994) Bacterivory and herbivory: key roles of phagotrophic protists in pelagic food webs. *Microb. Ecol.*, **28**, 223–235.

Sherr, E. B. and Sherr, B. F. (2007) Heterotrophic dinoflagellates: a significant component of microzooplankton biomass and major grazers of diatoms in the sea. *Mar. Ecol. Prog. Ser.*, **352**, 187–197.

Sherr, E. B. and Sherr, B. F. (2009) Capacity of herbivorous protists to control initiation and development of mass phytoplankton blooms. *Aquat. Microb. Ecol.*, **57**, 253–262.

Sieburth, J. M., Smetacek, V. and Lenz, J. (1978) Pelagic ecosystem structure: heterotrophic compartments of plankton and their relationship to plankton size fractions. *Limnol. Oceanogr.*, **23**, 1256–1263.

Smetacek, V. (1981) The annual cycle of protozooplankton in the Kiel Bight. *Mar. Biol.*, **63**, 1–11.

Smetacek, V. (2012) Making sense of ocean biota: how evolution and biodiversity of land organisms differ from that of the plankton. *J. Biosci.*, **37**, 589–607.

Smetacek, V., Klaas, C., Strass, V. H. *et al.* (2012) Deep carbon export from a Southern Ocean iron-fertilized diatom bloom. *Nature*, **487**, 313–319.

Smetacek, V. and Naqvi, S. W. A. (2008) The next generation of iron fertilization experiments in the Southern Ocean. *Philos. Trans. Roy. Soc. A*, **366**, 3947–3967.

Spindler, M., Hemleben, C., Bayer, U. *et al.* (1979) Lunar periodicity of reproduction in the planktonic forminifer *Hastigerina pelagica*. *Mar. Ecol. Prog. Ser.*, **1**, 61–64.

Strom, S. L. (2008) Microbial ecology of ocean biogeochemistry: a community perspective. *Science*, **320**, 1043–1045.

Strom, S. L., Macri, E. L. and Olson, M. B. (2007) Microzooplankton grazing in the coastal Gulf of Alaska: variations in top-down control of phytoplankton. *Limnol. Oceanogr.*, **52**, 1480–1494.

Strom, S. L. and Morello, T. A. (1998) Comparative growth rates and yields of ciliates and heterotrophic dinoflagellates. *J. Plankton Res.*, **20**, 571–584.

Takahashi, K. and Ling, H. Y. (1980) Distribution of *Sticholonche* (Radiolaria) in the upper 800 m of the waters in the Equatorial Pacific. *Mar. Micropaleontol.*, **5**, 311–319.

Throndsen, J. (1995) Estimating cell numbers. In Hallegraeff, G. M., Anderson, D. M. and Cembella, A. D. (eds), *Manual on Harmful Marine Microalgae*. UNESCO, Paris, pp. 63–80.

Trégouboff, G. (1957) Acantharia. In Trégouboff, G. and Rose, M. (eds), *Manuel de Planctonologie Méditerranéenne*. Centre National de la Recherche Scientifique, Paris, pp. 145–167.

Tsuda, A., Takeda, S., Saito, H. *et al.* (2003) A Mesoscale iron enrichment in the western Subarctic Pacific induces a large centric diatom bloom. *Science*, **300**, 958–961.

Zar, J. H. (2010) *Biostatistical Analysis*. 5th edn. Prentice Hall International, London.